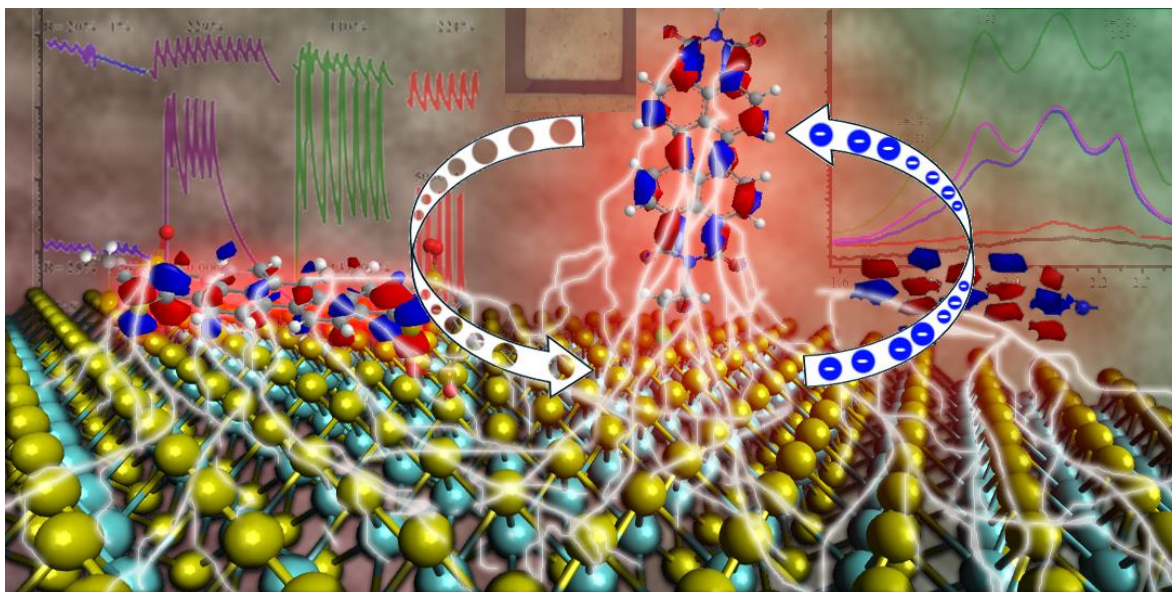


SUPPLEMENTARY INFORMATION



Covalent Functionalization Of Transition Metal Dichalcogenides With Perylene For Light Harvesting Devices

Ruben Canton-Vitoria, Yuki Matsunaga, Shaochun Zhang, Mengsong Xue, Minoru Osada, Ryo Kitaura.

Methods and techniques.

Chemical Vapor deposition (CVD) growing was carried out by using a separator temperature controller AFM-9P-III ASH and Argon flow was monitored by Horiba STEC controlled unit PE-D₂O.

Room-temperature PL spectra were measured by using a confocal Raman microscope (Renishaw InVia Raman and Horiba Jobin Yvon LabRAM HR-800) with 488, 633, 533 and 785 nm (max: 10 mW/cm² concentrated in 1 μm², 1200 or 2400 nm). All conditions were the same previous and after functionalization). A notch filter was used to filter out Rayleigh scattering, and Raman and PL signals were detected with a charge-coupled device (CCD). Ax 100 (0.8 NA) objective lens was used to focus the laser light on the samples. Low temperature measurements were performed in a home-made microscope employing lenses and filters and cryostats from ThorLABS for PL imaging, an LED light source (Mightex GCS-6500-15) was used to illuminate samples. PL intensity ($\lambda > 550$ nm) was imaged with CCD (Princeton Instruments PIXIS-1024BR-eXelon). PL spectra at a low temperature were performed with Princeton Instruments IsoPlane connected with CCD (Princeton Instruments PIXIS-1024BR-eXelon). In a cryostat Oxford cryogenic vacuum refrigerated with liquid Nitrogen/Helium. All vacuum systems reach values of 10⁻⁷ Torr by using a Pfeiffer vacuum chamber. Laser employed was a NKT photonics the power of light super extreme high power continuum white light laser connected to Princeton Instruments action spectrometer sp-2150 (The laser has a max intensity of 22 mW/cm² concentrated in 1 μm², 700, 1200 or 2400 nm). All conditions were the same previous and after functionalization) and the wavelength and intensity were calibrated with an IntelliCal from Princeton Instruments.

Electrochemical studies were recorded on an Autolab PGSTAT128N potentiostat/galvanostat equipped with a dual mode bipotentiostat (BA module) electrochemical analyser using a three-electrode system. For DPV, a glass carbon electrode was used as working electrode, a platinum cloth served as the counter electrode and a platinum wire was used as the reference electrode. The electrolyte was 0.1 M of tetrabutylammonium hexafluorophosphate and the solvent was dry DMF. All solutions were purged prior to electrochemical and spectral measurements using nitrogen gas for 15 minutes. Tetrabutylammonium hexafluorophosphate was crystallized 2 times before its use, as well as ferrocene. Ferrocene peak was calibrated to 0.0 V.

Atomic force microscope (AFM) observations were performed by the Veeco AFM system (Dimension 3100SPM, Nanoscope IV) operated at a scanning rate of (0.1-1) Hz.

High-resolution transmission electron microscopy (HRTEM) was performed on a JEOL JEM-2100F equipped with Energy Dispersive X-Ray (EDX) spectroscopy, working at 80 keV.

XPS TMDs grown on SiO₂/Si substrate were before or after functionalization with perylenes. Laser source employed was Al.

¹H NMR spectra were recorded in a 300 MHz Varian instrument operated by Vjnmr software, with TMS used as internal standard and CD₃Cl, deuterated DMSO or CS₂ as solvent. Steady-state UV-Vis electronic absorption spectra were recorded on a PerkinElmer (Lambda 19) UV-Vis-NIR spectrophotometer.

Lifetime were carried by using a single photon detection module ID-100-50-ULN from Becker and Hickler GMBH Nahmitzer.

All graphs were crafted using Origin 9.5 software and fitting or deconvolution usually shows values of $r^2=0.960-0.999$. Lifetime fitting was obtained towards decayFit and TEM image was processed by Gatan Digital Micrograph. AFM image was reconstructed by WSxM program and PL images by ImageJ. Transistor was performed using electron beam lithography irradiation instrument, with a channel of 5 μm and a length between 10-500 μm. Laser employed for the analysis of the photocurrents were 254 nm (10 mW/cm²), 365 nm (10 mW/cm²), 407 nm (30 mW/cm²), 532 nm (17 mW/cm²) and 650 nm (7 mW/cm²) with an aperture of 5 mm² using a fixed Pointer laser. Devices were measured using a Keithley semiconductor characterization.

Growth of CVD TMDs

Material	NaCl (%)	Precursor	mg	Oven 1	Oven 2	Oven 3	Flow (from oven 3 to oven 1)	Position boats on the tube and oven
MoS ₂ 2H	15	MoO ₃ /S	17	MO ₃ (1) 725 °C, 13 min. (2) 725 °C, 30 min. (3) 25 °C, 10 min	(1) 400 °C, 10 min. (2) 400 °C, 50 min.	Sulphur, 100 g (1) 0 °C, 12 min. (2) 210 °C, 10 min. (3) 210 °C 30 min.	(1) 250 ccm, 25 min. (2) 113 ccm.	
WS ₂ 2H	15	WO ₃ /S	10	WO ₃ (1) 780, °C 13 min. (2) 780, °C 30 min.	(1) 400 °C, 10 min. (2) 400 °C, 50 min.	Sulphur 100 g (1) 0 °C, 12 min. (2) 210 °C, 10 min. (3) 210 °C 30 min.	Argon at 113 ccm.	
MoSe ₂ 2H	17	MoO ₃ /Se (50/50%)	20	MO ₃ (1) 750 °C, 13 min. (2) 750 °C, 55 min.	Se (>200 g) (1) 350 °C, 12 min. (2) 370 °C, 10 min. (3) 410 °C, 16 min. (4) 425 °C, 15 min.	S (<3 mg) (1) 600 °C, 30 min. (2) 600 °C, 2 min.	Argon 400 ccm.	
WSe ₂ 2H	15	WO ₃ +Se (50/50%)	30	WO ₃ (1) 790 °C 13 min. (2) 795 °C 55 min.	Se (>200 g) (1) 350 °C, 12 min. (2) 370 °C, 10 min. (3) 410 °C, 16 min. (4) 425 °C, 15 min.	S (<3 mg) (1) 600 °C, 30 min. (2) 600 °C, 2 min.	Argon 400 ccm.	
MoTe ₂ 2H/1T	5	MoO ₃ (33%) Te (33%) MoCl ₆ (33%)	Spatula portion	MoO ₃ + Te + MoCl ₆ (1) 725 °C, 10 min. (2) 725 °C, 5 min. (3) 725 °C, 11 min. (4) 686 °C, 5 min. Include dry molecular sieves 0.4 A.	Te (1) 0 °C, 7 min. (2) 465 °C, 7 min. (3) 467 °C, until finish.		H ₂ , 30 ccm; Argon 100 ccm.	
MoO ₂	15	MoO ₃	60 mg	MO ₃ (1) 725 °C, 13 min. (2) 725 °C, 30 min. (3) 500 °C, 30 min.			Flow is 113 ccm.	
WO ₂	15	WO ₃	60 mg	WO ₃ (1) 780 °C, 13 min. (2) 780 °C, 30 min.			Argon 113 ccm 2 min later that reach 780 °C, connect the vacuum.	

Table S1. CVD synthesis.

Substrate treatment before CVD synthesis: SiO₂/Si substrates 6 x 2 cm² were washed in piranha solution for 15 minutes under sonication followed by 1 minute of sonication in ultrapure H₂O and MeOH. Then, substrates were dried using N₂ blowing and heated at 700 °C under an airflow of 400 ml/min for 30 minutes.

CVD synthesis: As example, MoS₂ (or WS₂) 15 mg of MoO₃ (or WS₂) containing 15% of NaCl was deposited at the centre of an alumina boat (10 x 1.5 cm²) with a height of 1.1 cm. The boats were put in a quartz tube with 3 cm in diameter. Argon gas was flowed with a flow rate of 113 ml/min, and MoO₃ was gradually heated up to 725 °C (780 °C) in 13 minutes. And then, Sulphur was also heated up to 210 °C in 10 minutes. All CVD parameters were kept constant for 30 additional minutes before a slow cooling down. All conditions can be described on table S1.

Liquid exfoliated MoS₂, MoSe₂, MoTe₂, WS₂, WSe₂ or WTe₂. Few grams of bulk were redispersed in DMAc and sonicated overnight. Supernatant were subtracted and filtrated with a 0.1 µm PTFE.

TEM grid preparation: A polypropylene carbonate (PPC) 15% in anisole film was spin-coated (5-seconds spinning at 1000 r.p.m followed by a 45-seconds coating at 6000 r.p.m) on a SiO₂/Si substrate with CVD-grown MoS₂ or WS₂; After heating at 135 °C for 1 minute, the SiO₂/Si substrate was soaked into water, and the PPC film was spontaneously separated from the substrate. The PPC film floating on the surface of water was directly scooped up with a TEM grid. After drying at room temperature, the TEM grid was annealed at 135 °C for 1 minute. Finally, the PPC film was dissolved in acetone overnight, and the resulting TEM grid was heated at 100 °C in vacuum for 30 minutes. After proper analysis the TMDs were functionalized with perylene as previously mentioned in the upper paragraph.

AFM. Few single layers of **1a** or **1b** were pick up of SiO₂/Si by employing a drop of dry PPC in a SiO₂/Si substrate. Then the specific flakes were transferred to a planar mechanically exfoliated multilayer h-BN on SiO₂, previously annealed. The PPC was dissolved in acetone overnight, and then completely purify by using DCM under Solhex reflux. Lately it was functionalized and carefully studied by PL and AFM analysis before and after functionalization.

PL emission: Experiments were carried out previous and after functionalization in SiO₂/Si substrate, since Perylene can intercalate between HBN layers masking results.

Device crafting. First photoresistor (ZEP520A) at room temperature were spin coated (1000 rpm 5 s and 6000 rpm 50 s) in pristine CVD-TMDs SiO₂/Si 270 nm. Later it was heated for 2 minutes a 180 °C in air and introduce in the EBL instrument. AutoCAD2020 and Wecas was employed to craft a pattern. Pattern were printed in few minutes (Parameters: 20KV; 5000pA; 10⁻⁴ Pa; 0.1seconds). Degraded ZEP520A polymer were lately removed by adding to the substrate O-xylene during 10 seconds in air.

Metal deposition of 20 nm of Bi and 50-80nm of Au were carried out by heating the metals in tungsten bouts at pressures between 2.3x10⁻⁸-2.5x10⁻⁶ Thors. On the other hand, the substrate was kept cold at 10 °C using water cooler system. Devices were obtained after lift-off in DMAc at room temperature by applying the minimal amount of pipetting. All devices were studied and functionalized with Perylene **1**. Then, its properties were once again studied.

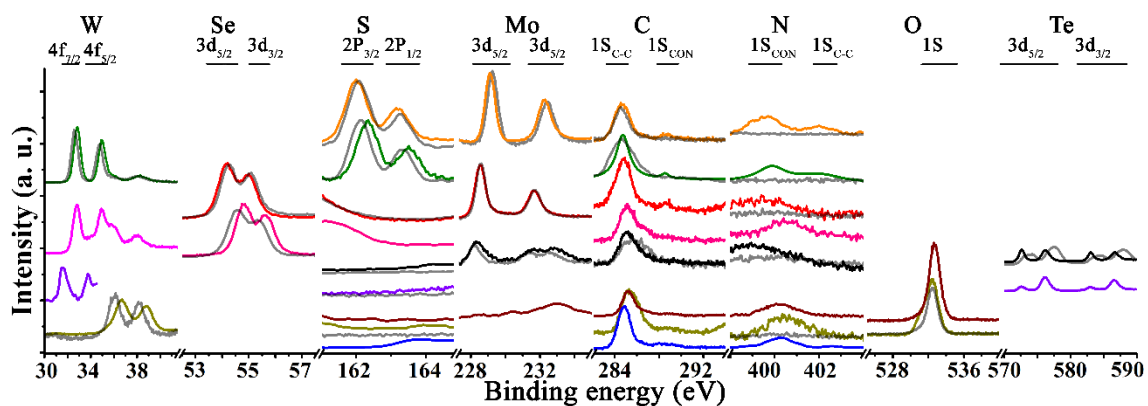


Figure S1. XPS spectra of TMDs: Per-MoS₂ (orange), Per-WSe₂ (olive), Per-MoSe₂ (red), Per-WSe₂ (pink), Per-MoTe₂ (black), Per-WTe₂ (purple), Per-MoO₂ (wine), Per-WO₂ (dark yellow), and perylene (blue), showing the W 4f, Se 3d, S 2p, Mo 3d, C 1s, N 1s, O 1s, and Te 3d orbitals.

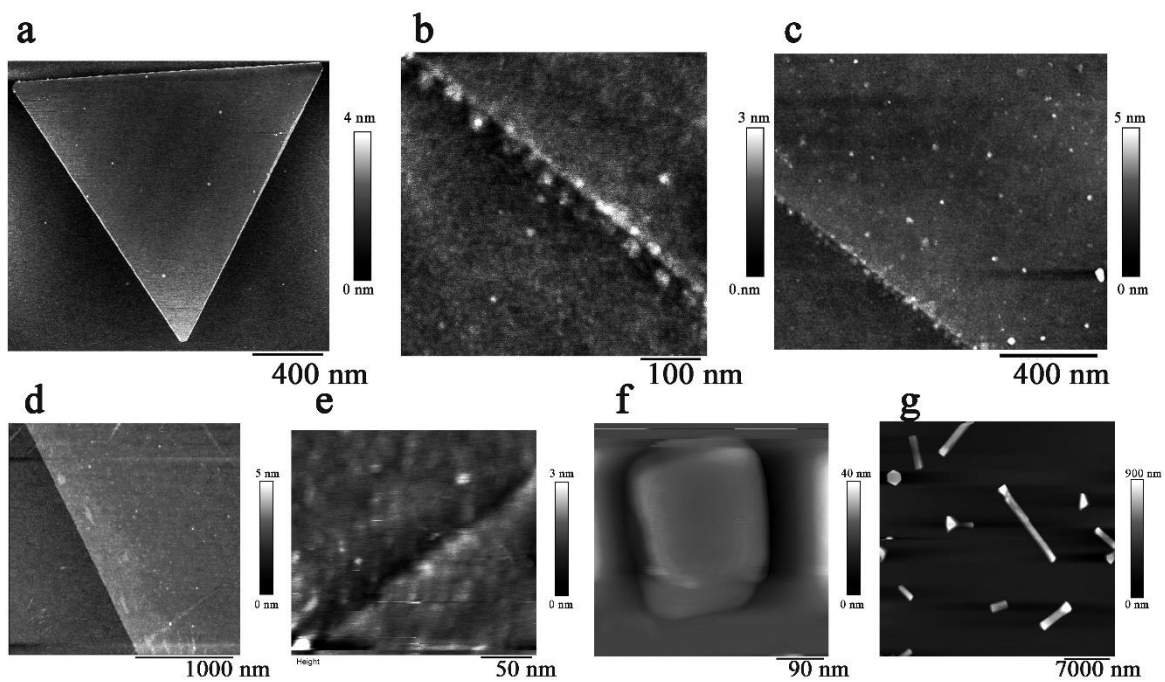


Figure S2. Per-TMDs after annealing at 600 °C, in presence of the corresponding chalcogen and with an argon flow of 300 ccm for (a) MoS₂, (b) WS₂, (c) MoSe₂ and (d) WSe₂, and pristine materials for (e) MoTe₂, (f) MoO₂, (g) WO₂.

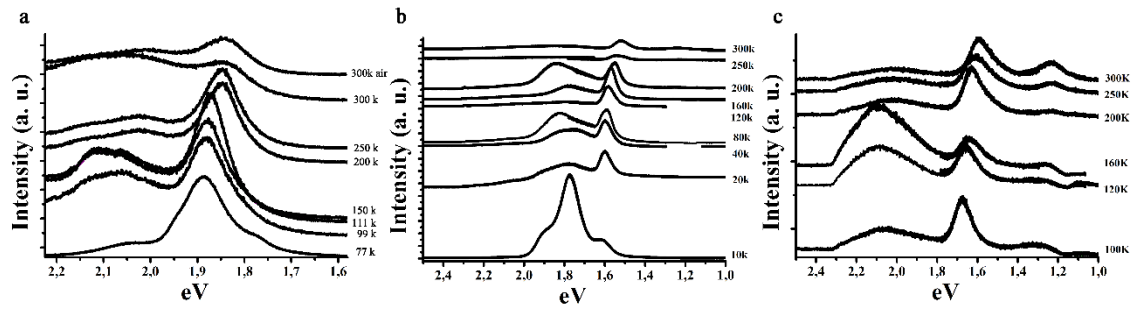


Figure S3. PL emission of (a) Per-MoS₂, (b) Per-MoSe₂, and (c) Per-WSe₂ at different temperatures, at 488 nm laser excitation and powers of 1.4 mW/cm² concentrated in a few microns.

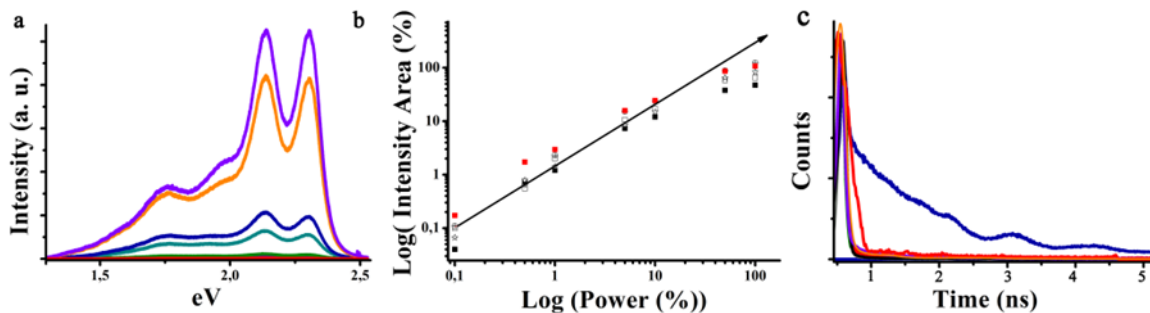


Figure S4. (a and b) PL emission of Per-WS₂ at 80 K under different incident laser powers, at 488 nm laser excitation. The full laser power was 10 mW/cm², focused on a spot with a diameter of 1 μm. (c) Fluorescence lifetime decay (Lineal scale; 1000 counts) of Perylene (blue), Per-MoS₂ (orange), IRF (grey), Per-WS₂ (olive), Per-MoSe₂ (red), Per-WSe₂ (pink), Per-MoTe₂ (black), Per-WTe₂ (purple).

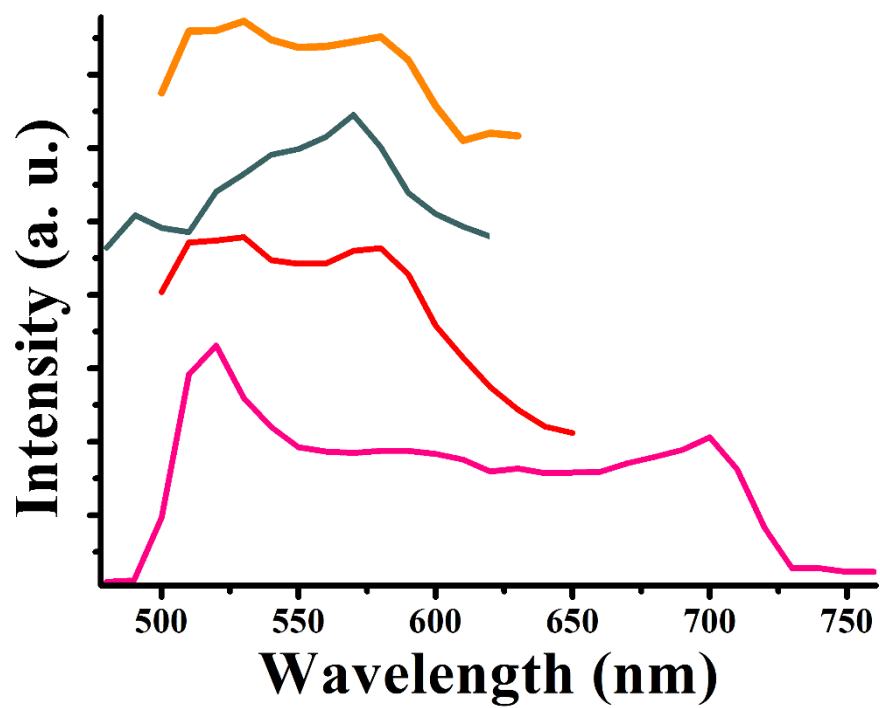


Figure S5. PLE of Per-MoS₂ (orange), Per-WS₂ (deep blue), Per-MoSe₂ (red), and Per-WSe₂ (pink).

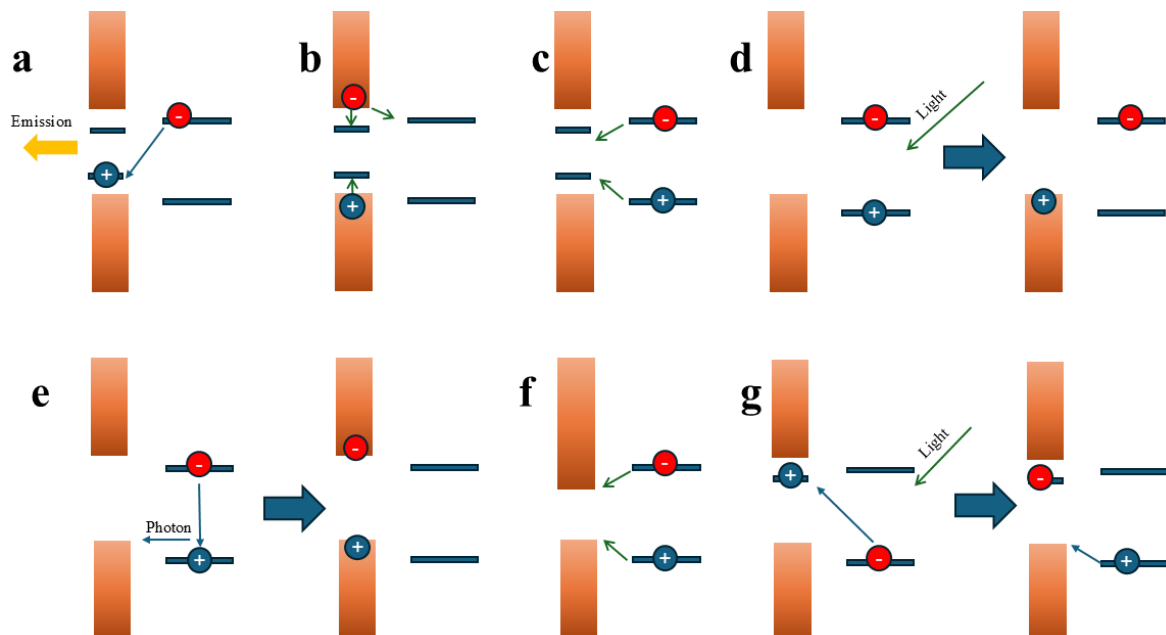


Figure S6. Electronic processes involved in (a) the formation of new NIR bands in Per-WS₂ and Per-MoSe₂ and Per-WSe₂. Depletion of carrier mobilities for (b) semiconducting TMDs (except MoTe₂) under dark conditions or in the absence of perylene irradiation. (c) Depletion of spontaneously generated excitonic species in perylene by trap states of TMDs, under dark conditions. Carrier injection by perylene through (d) electron transfer in semiconducting TMDs (except MoTe₂) and (e) energy transfer in semiconducting TMDs under perylene light excitation. (f) Carrier injection by perylene in MoTe₂ under perylene light excitation. (g) Plausible explanation for the enhancement of carriers in WS₂ at energies lower than the perylene excitation.

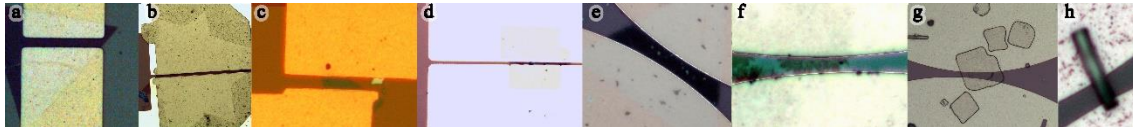


Figure S7. Optical microscope showing the channel of (a) Per-MoS₂, (b) Per-WS₂, (c) Per-MoSe₂, (d) Per-WSe₂, (e) Per-MoTe₂, (f) Per-WTe₂, (g) Per-MoO₂, (h) Per-WO₂.

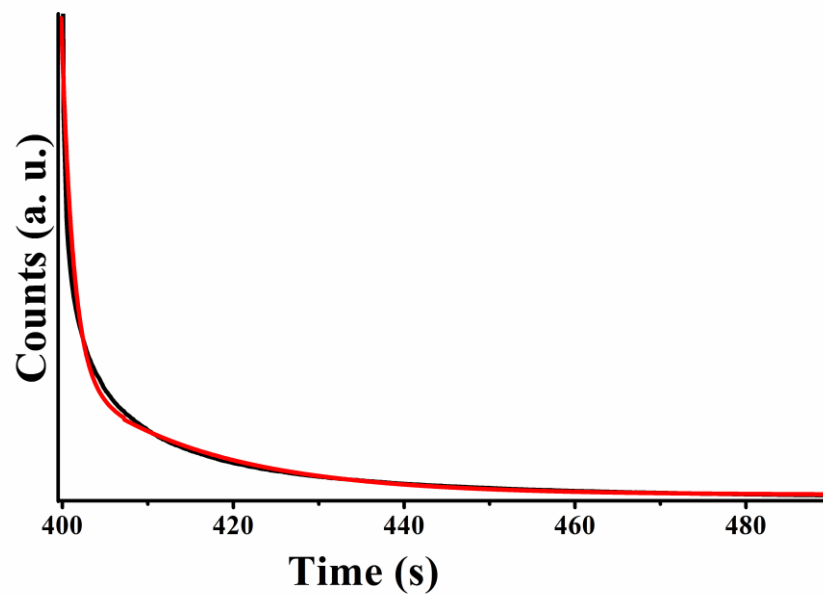


Figure S8. Representative photo-response-lifetime recovery of Per-WS₂.

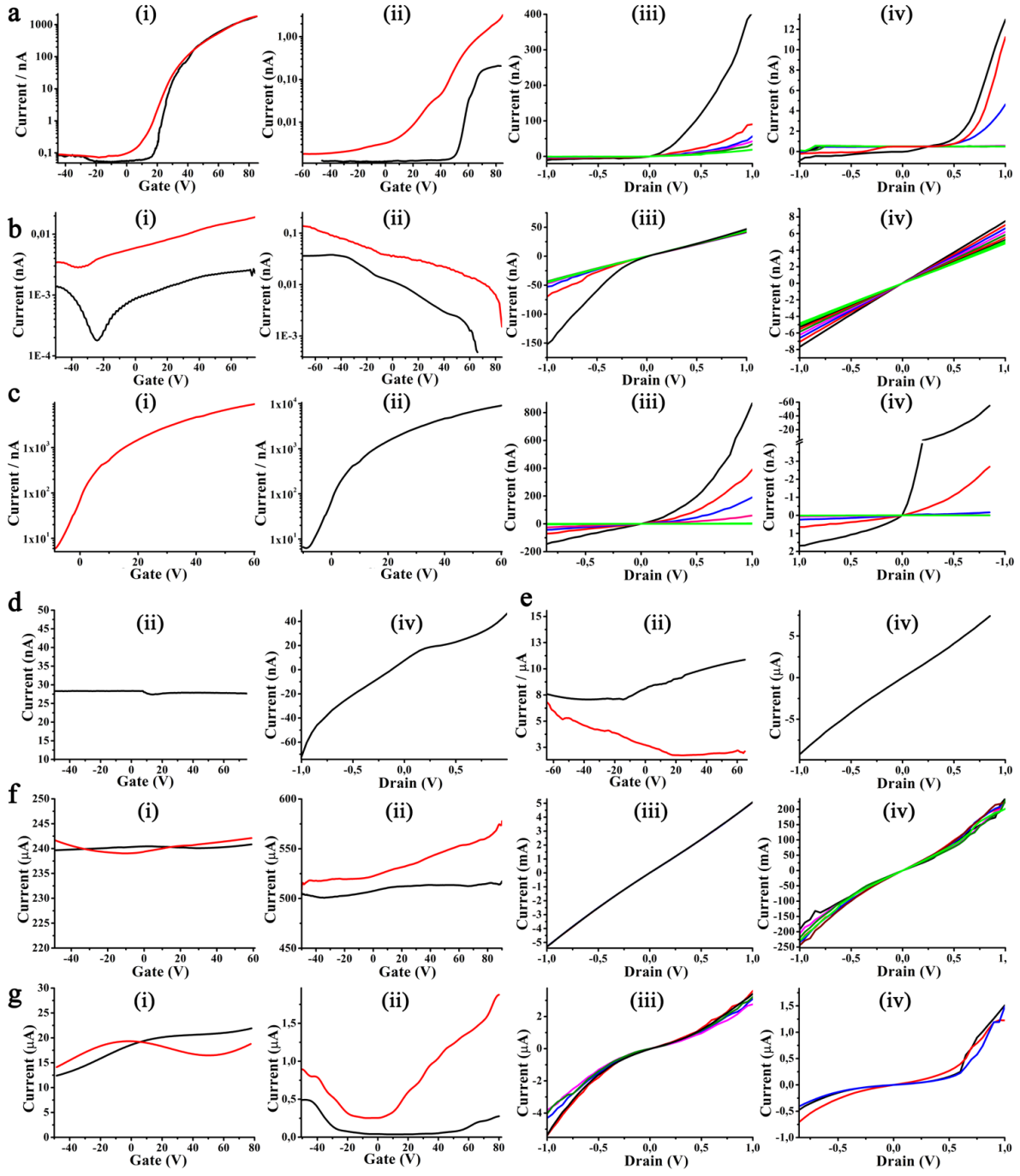


Figure S9. Transfer curves for pristine TMDs (i) and Per-TMDs (ii), and output characteristics for pristine TMDs (iii) and Per-TMDs (iv), for TMDs involving (a) WS₂, (b) MoSe₂, (c) WSe₂, (d) MoTe₂, (e) WTe₂, (f) MoO₂, and (g) WO₂.

PHOTO-RESPONSE (%)								
λ (nm)	MoS ₂	MoSe ₂	MoTe ₂	WS ₂	WSe ₂	WTe ₂	MoO ₂	WO ₂
254	154		0	2025	142	0	0	0
354	12	0	0	49	92	0	0	0
407	273	4488	0	1650	8362	0	0	0
532	139	1276	0	5733	669	0	0	0
650	215	465	0	400	400	0	0	0
	Per-MoS ₂	Per-MoSe ₂	Per-MoTe ₂	Per-WS ₂	Per-WSe ₂	Per-WTe ₂	Per-MoO ₂	Per-WO ₂
254	23	633	0.9	608	200	0		0
354	25	5167	0	192	0	0	0	0
407	96391	165233	5.1	442	44900	-72	0	4.99
532	263057	14567	3.8	542	389900	-40	0	0
650	3672	64567	1.2	525	3900	100	0	0

Table S2. Photo-response of Per-TMDs materials under 254 nm (10 mW/cm²), 354 nm (10 mW/cm²), 407 nm (30 mW/cm²), 532 nm (17 mW/cm²), and 650 nm (7 mW/cm²) light irradiation, concentrated in an area of 0.5 cm². The incident area of the channel was determined from [Figure S7](#).

RESPONSIVITY (A/W)								
λ (nm)	MoS ₂	MoSe ₂	MoTe ₂	WS ₂	WSe ₂	WTe ₂	MoO ₂	WO ₂
254	2.70	0	0	1.27	1x10 ⁻⁴	0	0	0
354	0.21	0	0	0.0309	6x10 ⁻⁵	0	0	0
407	1.60	0.0333	0	0.345	0.0019	0	0	0
532	1.43	0.0167	0	2.12	0.000268	0	0	0
650	5.39	0.0148	0	0.359	0.000389	0	0	0
λ (nm)	MoS ₂	MoSe ₂	MoTe ₂	WS ₂	WSe ₂	WTe ₂	MoO ₂	WO ₂
254	0.000681	0.000249	10.5	0.00382	2x10 ⁻⁶	0	0	0
354	0.000759	0.00203	0	0.00120	0	0	0	0
407	0.959	0.0216	20.1	0.000925	0.000157	-0.00157	0	0.000770
532	4.62	0.00337	26.2	0.00200	0.00240	-0.00154	0	0
650	0.157	0.0362	19.7	0.00471	5x10 ⁻⁵	0.00935	0	0

Table S3. Responsivity of Per-TMDs materials under 254 nm (10 mW/cm²), 354 nm (10 mW/cm²), 407 nm (30 mW/cm²), 532 nm (17 mW/cm²), and 650 nm (7 mW/cm²) light irradiation, concentrated in an area of 0.5 cm². The incident area of the channel was determined from [Figure S7](#).

EQE (%)								
λ (nm)	MoS ₂	MoSe ₂	MoTe ₂	WS ₂	WSe ₂	WTe ₂	MoO ₂	WO ₂
254	1316	0	0	621	0.0473	0	0	0
354	73.4	0	0	10.8	0.0220	0	0	0
407	487	10	0	105	0.578	0	0	0
532	334	3.9	0	494	0.0624	0	0	0
650	1027	2.8	0	68.5	0.0742	0	0	0
λ (nm)	MoS ₂	MoSe ₂	MoTe ₂	WS ₂	WSe ₂	WTe ₂	MoO ₂	WO ₂
254	0.332	0.121	5112	1.87	0.00102	0	0	0
354	0.266	0.711	0	0.422	0	0	0	0
407	292	6.59	6115	0.282	0.0477	-0.479	0	0.235
532	1076	7.84	6109	0.467	0.560	-0.359	0	0
650	30	6.91	3753	0.899	0.0111	1.78	0	0

Table S4. External quantum efficiency of Per-TMDs materials under 254 nm (10 mW/cm²), 354 nm (10 mW/cm²), 407 nm (30 mW/cm²), 532 nm (17 mW/cm²), and 650 nm (7 mW/cm²) light irradiation, concentrated in an area of 0.5 cm². The incident area of the channel was determined from [Figure S7](#).

SPECIFIC DETECTIVITY (Jones)								
$\lambda(\text{nm})$	MoS ₂	MoSe ₂	MoTe ₂	WS ₂	WSe ₂	WTe ₂	MoO ₂	WO ₂
254	2.5x10 ¹⁰	0	0	1.3 x10 ¹¹	2.3 x10 ⁸	0	0	0
354	2.0x10 ⁹	0	0	3 x10 ⁹	1.5 x10 ⁸	0	0	0
407	1.5x10 ¹⁰	5.6 x10 ⁹	0	3 x10 ¹⁰	4.5 x10 ⁹	0	0	0
532	1.4x10 ¹⁰	2.8 x10 ⁹	0	2.2x10 ¹¹	6.3 x10 ⁸	0	0	0
650	5x10 ¹⁰	2.5 x10 ⁹	0	3.8 x10 ¹⁰	9.2 x10 ⁸	0	0	0
$\lambda(\text{nm})$	MoS ₂	MoSe ₂	MoTe ₂	WS ₂	WSe ₂	WTe ₂	MoO ₂	WO ₂
254	1.6x10 ⁸	3.2x10 ⁸	7.9x10 ⁸	4.0 x10 ⁹	4.0 x10 ⁷	0	0	0
354	1.7x10 ⁸	2.6x10 ⁹	0	1.1 x10 ⁹	0	0	0	0
407	2.2 x10 ¹¹	2.8x10 ¹⁰	1.5 x10 ⁹	1.0x10 ⁹	3.0 x10 ⁹	-1.8 x10 ¹⁰	0	4.6 x10 ⁸
532	1.1 x10 ¹²	4.3x10 ⁹	2.0 x10 ⁹	2.1 x10 ⁹	4.6 x10 ⁹	-1.7x10 ¹⁰	0	0
650	3.6 x10 ¹⁰	4.6x10 ¹⁰	15 x10 ⁹	5.0 x10 ⁹	1.2 x10 ⁹	1.0x10 ¹¹	0	0

Table S5. Specific detectivity of Per-TMDs materials under 254 nm (10 mW/cm²), 354 nm (10 mW/cm²), 407 nm (30 mW/cm²), 532 nm (17 mW/cm²), and 650 nm (7 mW/cm²) light irradiation, concentrated in an area of 0.5 cm². The incident area of the channel was determined from [Figure S7](#).

TRANSCONDUCTANCE (A/V)								
	MoS ₂	MoSe ₂	MoTe ₂	WS ₂	WSe ₂	WTe ₂	MoO ₂	WO ₂
Dark	3.8x10 ⁻⁷	3.2x10 ⁻¹⁴		5.2x10 ⁻⁸	2.3x10 ⁻⁷			
532 nm	-7.4x10 ⁻⁷	2.9x10 ⁻¹³		6.2x10 ⁻⁸				
	Per-MoS ₂	Per-MoSe ₂	Per-MoTe ₂	Per-WS ₂	Per-WSe ₂	Per-WTe ₂	Per-MoO ₂	Per-WO ₂
Dark	4.3x10 ⁻⁸	-9.3x10 ⁻¹³		2.1 x10 ⁻¹¹	2.3x10 ⁻⁷	3.7x10 ⁻¹²		1.3x10 ⁻⁸
532 nm	9.0x10 ⁻⁶	4.7x10 ⁻¹²		3.3 x10 ⁻¹¹		-4.0x10 ⁻¹⁰		4.3x10 ⁻⁸
CARRIER MOBILITY (cm ² /V·S)								
	MoS ₂	MoSe ₂	MoTe ₂	WS ₂	WSe ₂	WTe ₂	MoO ₂	WO ₂
Dark	0.73	9.41 x10 ⁻⁷	0	0.141	0.96			
532 nm	7.6	8.6 x10 ⁻⁶		0.169				
	Per-MoS ₂	Per-MoSe ₂	Per-MoTe ₂	Per-WS ₂	Per-WSe ₂	Per-WTe ₂	Per-MoO ₂	Per-WO ₂
Dark	0.45	2.7 x10 ⁻⁵	0	5.8 x10 ⁻⁵	0.96	3.4 x10 ⁻¹⁰		1.20
532 nm	93	1.4 x10 ⁻⁴		9.0 x10 ⁻⁵		3.7 x10 ⁻⁸		4.22

Table S6. Transconductance and carrier mobility of Per-TMDs materials under dark and 532 nm (17 mW/cm²) excitation. The incident area of the channel was determined from [Figure S7](#).

Conductivity (nS/sq)								
λ (nm)	MoS ₂	MoSe ₂	MoTe ₂	WS ₂	WSe ₂	WTe ₂	MoO ₂	WO ₂
Dark	8.770	0.0272	0.0134	0.0710	0.000138	0.0000001	344444444	452.5
254	22.251	0.0272	0.0134	1.509	0.000334	0.0000001	344444444	452.5
354	9.817	0.0272	0.0134	0.106	0.000265	0.0000001	344444444	452.5
407	32.723	1.248	0.0134	1.242	0.0117	0.0000001	344444444	452.5
532	20.943	0.3744	0.0134	4.141	0.00106	0.0000001	344444444	452.5
650	27.617	0.1536	0.0134	0.355	0.000689	0.0000001	344444444	452.5
	Per-MoS ₂	Per-MoSe ₂	Per-MoTe ₂	Per-WS ₂	Per-WSe ₂	Per-WTe ₂	Per-MoO ₂	Per-WO ₂
Dark	0.0149	0.00048	5535.048	0.000710	2.12x10 ⁻⁶	0.00000025	344444444	0.00221
254	0.0183	0.00352	5583.92	0.00503	6.36 x10 ⁻⁶	0.00000025	344444444	0.00221
354	0.0187	0.0253	5535.048	0.00207	2.12 x10 ⁻⁶	0.00000025	344444444	0.00221
407	14.398	0.7936	5816.077	0.00385	0.000955	0.00000007	344444444	0.113
532	39.267	0.0704	5743.010	0.00456	0.00827	0.00000015	344444444	0.00221
650	0.563	0.3104	5599.318	0.00444	8.48x10 ⁻⁵	0.00000005	344444444	0.00221

Table S7. Conductivity of Per-TMDs materials under dark and 254 nm (10 mW/cm²), 354 nm (10 mW/cm²), 407 nm (30 mW/cm²), 532 nm (17 mW/cm²), and 650 nm (7 mW/cm²) light irradiation, concentrated in an area of 0.5 cm². The incident area of the channel was determined from [Figure S7](#).

Formulas

We evaluated the optical bandgap via Varshini equation.

$$Eq.S1: E(T) = E(0) - \frac{\alpha T^2}{T+\beta}$$

Where T is the temperature in kelvin, $E(T)$ and $E(0)$ are the optical gaps at a specific temperature and zero kelvin respectively. Then, α and β are fitting parameters.

In addition, the photo-response (R), responsivity (R_λ), the external quantum efficiency (EQE), detectivity (D^*), transconductance (G_m), carrier mobility (μ) and superficial conductivity (σ_{sq}) employed for pristine TMDs and Per-TMDs materials are shown below, as eq. S2-S8 respectively.

$$Eq.S2: R(\%) = \frac{I_{Ligth} - I_{dark}}{I_{dark}} \times 100$$

$$Eq.S3: R_\lambda = \frac{\Delta I}{AP_i}$$

$$Eq.S4: EQE(\%) \approx \frac{1240 \times R_\lambda}{\lambda}$$

$$Eq.S5: D^* = \frac{R_\lambda}{\sqrt{A \times I_{dark}}}$$

$$Eq.S6: G_m = \frac{\Delta I}{\Delta V_g}$$

$$Eq.S7: \mu = \frac{L}{WC_{ox}} \times \frac{G_m}{V_{DS}}$$

$$Eq.S8: \sigma_{sq} = \frac{L \times I_{DS}}{W \times V_{DS}}$$

Wherein I_{DS} is the current between the drain and source. I_{Ligth} and I_{dark} are I_{DS} under light and dark illumination, respectively, and ΔI is a variation of I_{DS} under dark and light illumination. λ is the wavelength of the excitation laser, P_i is the incident power density, A is the active area of the photodetector and ΔV_g is the variation of the gate voltage. In addition, L and W are the length and the width of the device, and V_{DS} is the drain to source voltage. C_{ox} is the capacitance per unit area of SiO₂ 270 nm, corresponds to a value of 12.79 nF/cm².